Analysis of Noise Origin in Ultra Stable Resonators: Preliminary Results on Measurement Bench

Fabrice Sthal, Serge Galliou, Xavier Vacheret, *FEMTO-ST Frequency and Time Department*
Patrice Salzenstein, R. Brendel, E. Rubiola, *FEMTO-ST Frequency and Time Department*
G. Cibiel, *CNES Microwave and Time-Frequency Department*

INTRODUCTION

The Centre National d'Etudes Spatiales (CNES), Toulouse, France and FEMTO-ST Institute, Besancon, France, have initiated a program of investigations on the origins of noise in bulk acoustic wave resonators. Several European manufacturers of high quality resonators and oscillators take part in this operation [1].

Tests and measurements are mainly performed on an advanced phase noise measurement system, recently set up for this program [2].

Investigations on the sensitivity of selected quartz crystal resonators to various externally-controlled parameters such as temperature, drive level, load impedance, and series capacitance are presented. Various batches of different types of 5 and 10 MHz quartz crystal resonators provided by the industrial partners have already been tested (conventional, QAS, BVA, …).

PRINCIPLE OF THE MEASUREMENT BENCH

The bench principle uses carrier suppression technique [3-4]. The general idea of this passive method (Fig. 1) consists in reducing the noise of the source as much as possible.

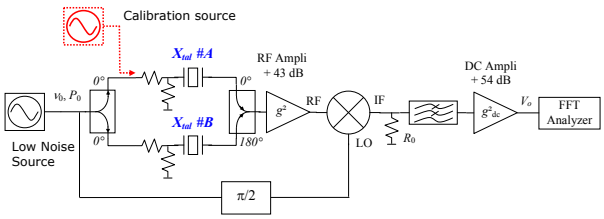

Figure 1. Principle of the measurement bench.

Indeed, when resonators exhibit a very weak noise, the noise of the source is always higher than that of the quartz crystal resonator. Thus, the direct feeding of the driving source signal through only one resonator does not permit to extract the resonator noise from the output resulting noise. On the other hand, the source signal can be subtracted when passing through two identical arms equipped with identical resonators (the devices under tests: DUT). Then the contribution of the source is cancelled while inner noise of both resonators is preserved because one resonator noise is different from the other one. When the carrier suppression is achieved (less than -75 dBc is acceptable), the resulting signal only made up noise from both resonators, is strongly amplified and mixed with the source signal to be shifted down to the low frequency domain and processed by the spectrum analyzer. In such a way, noise to be measured from both resonators can be brought up at a higher level than the driving source noise. Moreover, the noise floor of the bench can be measured with resistors substituted for crystal resonators.

Fig. 2 shows the measurement system. The new bench developed here has been obtained from two previous systems used in our laboratory experiences [3-4].

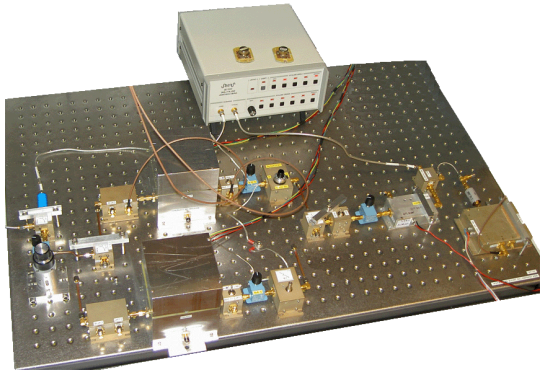

Figure 2. Measurement bench of resonator phase noise.

Calibration of the measurement system is obtained by injecting a known side band on one of the arms of the bridge. The noise of the DUT, as seen on the fast Fourier transform analyzer, is corrected using the calibration factor determined with the side band.

The input power of the bench comes from a synthesizer referenced to an ultra-stable OCXO. It is used at a typical power level. The power adjustment in the bench is realized by step attenuators. The crystal dissipated power can be moved from a few µW to approximately 200 µW. Each resonator is driven in the bench arm through an input resistance network matched to 50 Ω impedance. This network is composed of two resistances and depends on the motional resistance of the resonator. They are soldered near the resonator and inside the oven. The resonator is associated with a tuning capacitor to get the resonance of the resonator at the source frequency. But, in our configuration, the frequency tuning can be done also with the synthesizer frequency at a constant tuning capacitor. The tuning method can be chosen according to the observed phenomenon.

PRELIMINARY RESULTS

1. *Noise floor of the bench*

The scientific program implies measurements according to the crystal dissipated power. To get 200 µW inside the resonator, the input power of the bench should be sufficient to take into account the insertion loss.

Before resonator measurements, the noise floor of the bench has been studied according to the output power of the synthesizer. The DUT dissipated power is maintained constant by tuning the input attenuator of the bench. Fig. 3 shows the monolateral power spectral density of the phase fluctuations $\mathcal{L}(f)$ versus the Fourier frequency with the synthesizer output power as a parameter.

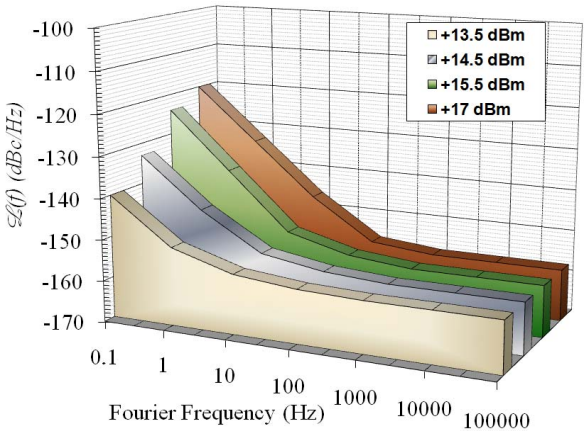

Figure 3. Noise floor of the measurement system.

Below 100 Hz, the noise floor goes up when the output power of the synthesizer increases. The synthesizer output power must be under 15.5 dBm to get a floor below – 140 dBc/Hz at an offset frequency of 1 Hz.

The insertion loss between the bench input and the resonator input has a minimum value of -8.2 dB. Thus, with a synthesizer output power of +15.5 dBm, the maximum input power into the resonator is 7.3 dBm. If the motional resistance of the resonator is around 50 Ω, the maximum of the crystal dissipated power is about 215 µW.

2. *Resonator classification*

Various resonator batches issued from different processes, namely from A to E, are compared in Fig. 4. The Allan standard deviation is given according to the quality factor of the quartz crystals. The driving power is identical to the one used in oscillator. Results are presented by resonator pairs when considering both quartz non identical.

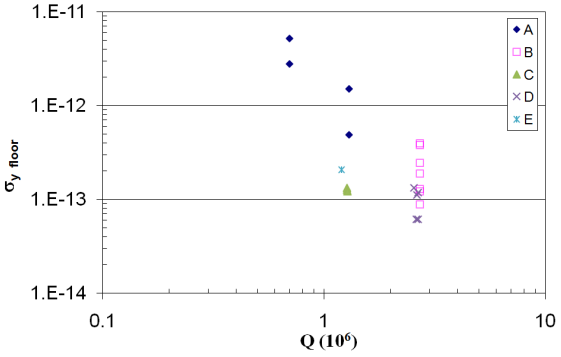

Figure 4. Allan standard deviation floor of the resonator pairs issued from different manufacturer batches.

3. *Influence of the tuning capacitor*

a) *Theoretical aspect*

The classical equivalent circuit of a resonator is given in Fig. 5. R_x, C_x and L_x are the motional parameters of the resonator and C_0 is the static capacitor.

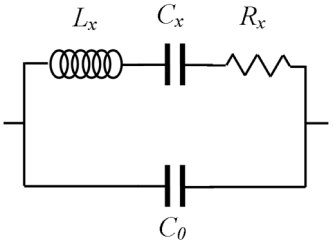

Figure 5. Electrical model of a crystal resonator whose motional parameters are L_x, C_x and R_x. C_0 is its parallel capacitor.

In the measurement system, the resonator frequency has always to be tuned. Into each arm of the bench, as in an oscillator, this is fulfilled by a series capacitor having a pull-up effect, here so-called tuning capacitor C_t. Moreover, the resonator is inserted in an impedance matching π network (Fig. 6).

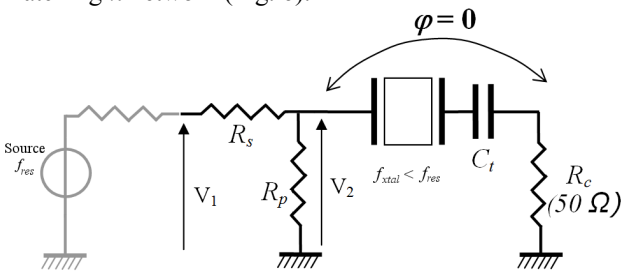

Figure 6. Electrical circuit of one arm of the bench. C_t denotes the tuning series capacitor added to pull-up the overall resonant frequency.

Classically, the resulting frequency is given with a good approximation by [1]:

$$f_{res} \approx f_{xtal}\sqrt{1+\frac{C_x}{C_0+C_t}} \qquad (1)$$

At the resonance frequency, the overall system presented in Fig. 6 is equivalent to the one shown in Fig. 7.

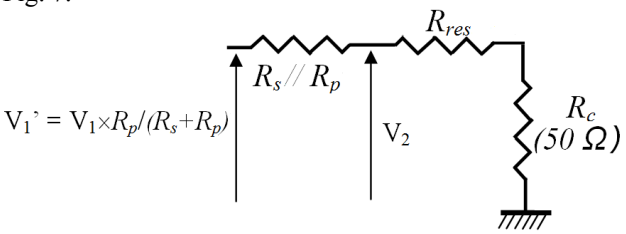

Figure 7. Equivalent circuit of one arm of the bench.

R_{res} is the equivalent résistance of the resonator and its tuning capacitor and depends on C_t as:

$$R_{res} = R_x\left(1+\frac{C_0}{C_t}\right)^2 \qquad (2)$$

Thus, the resonator dissipated power P_{xtal} is a function of the tuning capacitor C_t. P_{xtal} is given according to C_t in Fig. 8 for a resonator with classical motional parameters, R_x = 50 Ω and C_0 = 5 pF. An optimum value of C_t, C_{tPmax},

can be observed versus P_{xtal}. It corresponds to the impedance matching. In this case, R_{res} is equal to the total load R_L given by:

$$R_L = R_c + (R_s \,//\, R_p) \qquad (3)$$

And,

$$C_{tP\max} = C_0 \times \frac{1}{\sqrt{\frac{R_L}{R_x} - 1}} \qquad (4)$$

Thus, the loaded quality factor of the resonator is equal to fifty percent of the unloaded one. The zero crossing of the derivative of P_{xtal} is clearly identified in Fig. 9. P_{xtal} becomes really sensitive to C_t variations for capacitor values which are less than the optimum one.

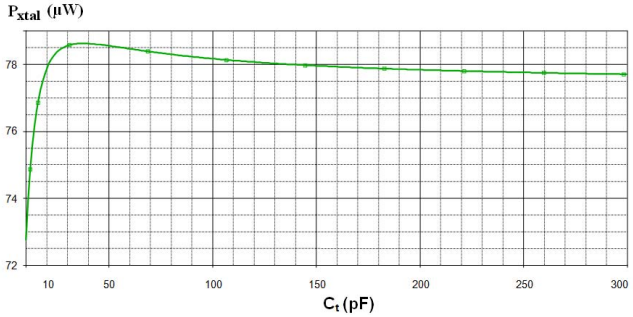

Figure 8. Dissipated power in the resonator for an input level V'_1 = 300 mV. Resonator parameters: R_x = 50 Ω and C_0 = 5 pF.

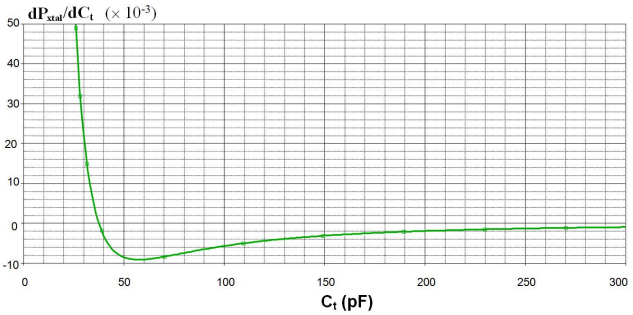

Figure 9. Derivative to C_t of the resonator dissipated power. The derivative is equal to 0 for C_t = 37.5 pF.

This simple modelization shows that the tuning capacitor C_t should not be chosen lower than C_{tPmax}. $C_t = C_{tPmax}$ is the best configuration or a value $C_t >> C_{tPmax}$ is also another possibility.

b) *Measurements*

Capacity values have been chosen according to the previous discussion at 10 pF, 60 pF and 220 pF. Fig. 10 illustrates the frequency shift induced by the serial capacitor. In this case, the considered resonator is a classical 10 MHz SC cut quartz crystal.

Allan standard deviation of a 10 MHz, SC cut, resonator is given according to C_t in Fig. 11. All noise values are inside the error bars except for the smallest value of C_t.

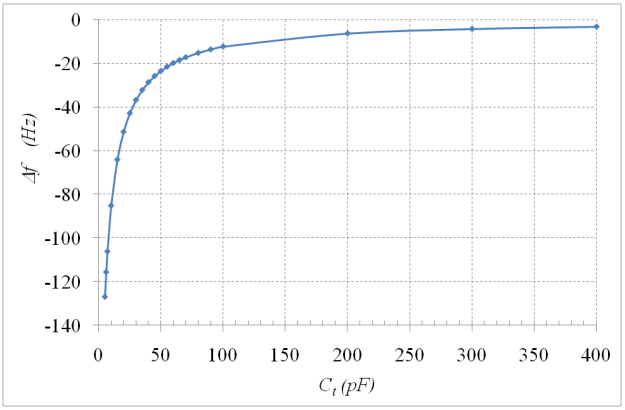

Figure 10. Frequency shift versus C_t of a 10 MHz, SC-cut resonator.

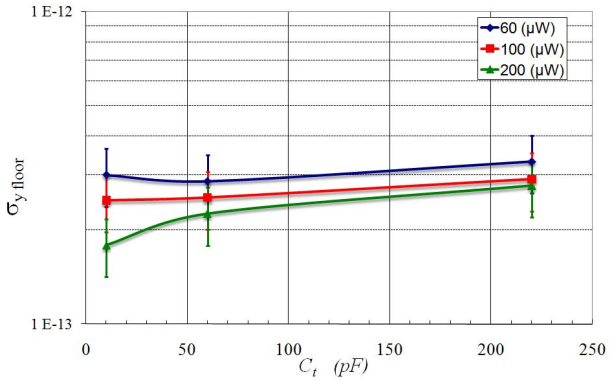

Figure 11. Allan standard deviation according to C_t.

4. *Crystal dissipated power*

Measurements have been carried out on five 10 MHz, SC-cut, quartz crystal resonator pairs of a manufacturer A. As the resonator dissipated power in oscillator is 100 µW, the measurement power is varied to 20, 100 and 200 µW. The tuning capacitor C_t remains constant when power is changed. The frequency shift induced by the amplitude frequency effect is compensated by the source frequency of the synthesizer. Fig. 12 shows the Allan standard deviation drawn versus the crystal dissipated power P_{xtal}. For these 10 MHz resonators, C_t is equal to 60 pF.

Three, 5 MHz, SC-cut, BVA resonators of manufacturer B have been also measured according to the crystal dissipated power (Fig. 12). C_t is equal to 33 pF. The trend of the curve is similar to the 10 MHz resonator one. Unfortunately measurements up to 100 µW have not been done in order to keep safe these resonator pairs.

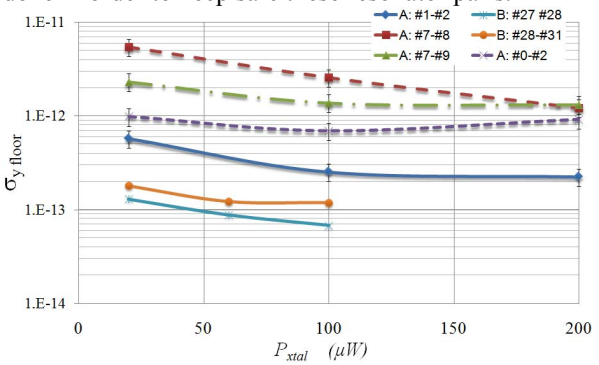

Figure 12. Allan standard deviation according to crystal dissipated power.

Fig. 13 shows the Allan standard deviation of the best 10 MHz, SC-cut, resonator pairs (A: #1-#2). σ_{yfloor} has been measured for two supplementary values of P_{xtal}. The first one is measured, between 20 µW and 100 µW, and the second one between 100 µW and 200 µW. The values remain in the measurement error and follow the previous trend.

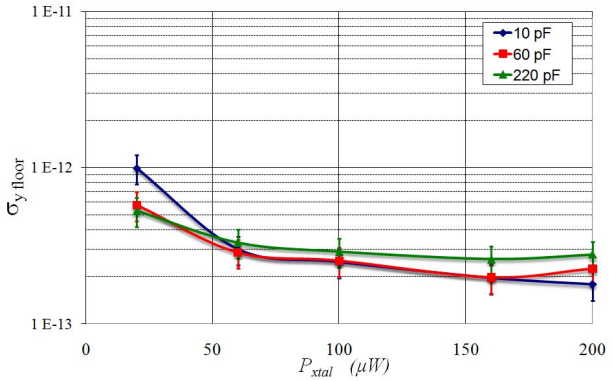

Figure 13. Allan standard deviation according to the resonator dissipated power for the resonator pair A:#1-#2.

5. *Influence of the turnover temperature*

The influence of the temperature is particularly studied according to the operating point versus the quartz crystal turn over temperature. A double enclosure and two thermally controlled ovens are used in order to control the quartz crystal temperature. The temperature step can be lower than 0.05°C between two remote-controlled operating temperatures around 70 °C [5]. This kind of oven is equivalent to double ovens used in ultrastable oscillators.

Noise measurements have been done on classical 10 MHz, SC-cut quartz crystal resonator. Resonators are not self suspended and with adherent electrodes. This kind of resonator can be considered as most temperature sensitive as the QAS or BVA ones.

Fig. 14 shows the frequency temperature behaviour of the quartz crystal resonator.

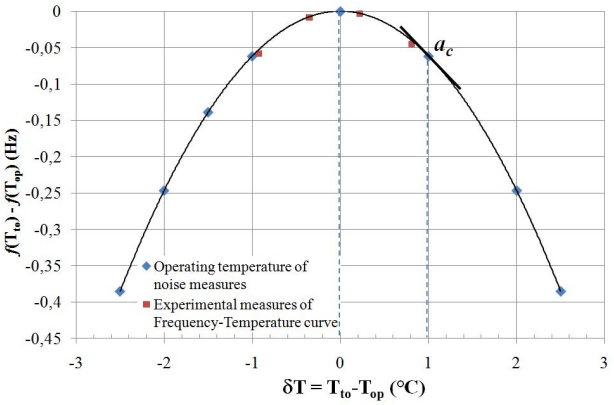

Figure 14. Frequency temperature behavior of the SC-cut quartz crystal at 10 MHz.

The ideal operating point for a quartz crystal in C-mode is the temperature T_{to} of its turnover point. The turnover temperature of the considered resonator is equal to 69.7 °C. In our experiments, the operating temperature T_{op} is moved around the turnover point. As a consequence, the relative frequency variation of the resonator is given by:

$$\frac{\Delta f}{f} = a_{c)T_{op}} \times \Delta T_{oven}$$

Where ΔT_{oven} is the oven stability, it is around 1.5 10^{-6} K [5]. The slope $a_{C)Top}$ is given by the derivative of the frequency-temperature behavior of the resonator at T_{op}.

Table 1 gives the relative frequency fluctuations due to the oven stability according to the temperature shift δT around T_{to}.

TABLE I. RELATIVE FREQUENCY FLUCTUATIONS ACCORDING TO THE TEMPERATURE SHIFT AROUND T_{TO}.

δT (°C)	-2.5	-2	-1.5	-1	0	1	2
a_c (10^{-8})	3	2.4	1.8	1.2	0	-1.2	-2.4
$\Delta f/f$ (10^{-14})	4.5	3.6	2.7	1.8	0	-1.8	-3.6

As expected frequency fluctuations induced by the temperature fluctuations are not visible in the resonator noise measurements (Fig. 15).

Fig. 15 shows that the modification of the temperature operating point has not a real influence on the resonator noise.

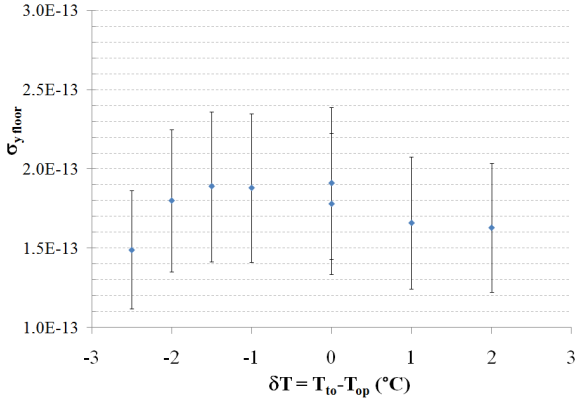

Figure 15. Allan standard deviation σ_{yfloor} of a resonator pair measured versus the temperature shift δT.

Dynamic effect analysis is now in progress. A small periodic modulation will be applied in T_{op}. The main difficulty of this experiment is the necessity to keep the output voltage in an acceptable range to make the noise measurement.

CONCLUSION

Several sets of measurements have been compared. The resonator noise is observed according to the input power in the bench arm. The resonator noise is also measured at constant resonator power according to a wide range of series capacitors. The tuning capacitor modifies the overall impedance, but, a correlation between load impedance, tuning capacitor and the flicker noise of the resonator is not shown. About the temperature influence, a stable oven allows to reject the relative frequency fluctuations due to the oven stability at a lower level than the quartz crystal noise. Because of the measurement errors, the resonator noise seems not influenced by the resonator operating temperature, but the trend of the curve is slightly disappointing. More measurements will be necessary to get a better understanding.

REFERENCES

[1] S. Galliou, F. Sthal, X. Vacheret, R. Brendel, P. Salzenstein, E. Rubiola and G. Cibiel, "*A program to analyze the origin of noise in ultra-stable quartz resonators*", Proc. Joint Meeting IEEE Ann. Freq. Cont. Symp. and European Frequency and Time Forum, Genova, Switzerland, 29 May-1 June, pp. 1176-1181, (2007).

[2] F. Sthal, X. Vacheret, P. Salzenstein, S. Galliou, E. Rubiola and G. Cibiel, "*Advanced bridge instrument for the measurement of the phase noise and of the short-term frequency stability of ultra-stable quartz resonators*", Proc. Joint Meeting IEEE Ann. Freq. Cont. Symp. and European Frequency and Time Forum, Genova, Switzerland, 29 May-1 June, pp. 254-260, (2007).

[3] F. Sthal, M. Mourey, F. Marionnet and W.F. Walls, "Phase noise measurements of 10 MHz BVA quartz crystal resonator", IEEE Trans. Ultrason. Ferroelec. Freq. Contr., vol. 47, p. 369-373, 2000.

[4] E. Rubiola, J. Groslambert, M. Brunet and V. Giordano, "Flicker noise measurement of HF quartz resonators", IEEE Trans. Ultrason. Ferroelec. Freq. Contr., vol. 47, p. 361-368, 2000.

[5] F. Sthal, S. Galliou, P. Abbe, X. Vacheret, G. Cibiel, *"New ultra stable crystal ovens and simple characterisation ",* Electronics Letters, vol. 43, no. 16, 2nd August, pp. 900-901, (2007).